Supramolecular Recognition

Deutsche Ausgabe: DOI: 10.1002/ange.201502045
Internationale Ausgabe: DOI: 10.1002/anie.201502045

Spatial, Hysteretic, and Adaptive Host–Guest Chemistry in a Metal–Organic Framework with Open Watson–Crick Sites**

*Hong Cai, Mian Li, Xiao-Rong Lin, Wei Chen, Guang-Hui Chen, Xiao-Chun Huang, and Dan Li**

Abstract: *Biological and artificial molecules and assemblies capable of supramolecular recognition, especially those with nucleobase pairing, usually rely on autonomous or collective binding to function. Advanced site-specific recognition takes advantage of cooperative spatial effects, as in local folding in protein–DNA binding. Herein, we report a new nucleobase-tagged metal–organic framework (MOF), namely ZnBTCA (BTC = benzene-1,3,5-tricarboxyl, A = adenine), in which the exposed Watson–Crick faces of adenine residues are immobilized periodically on the interior crystalline surface. Systematic control experiments demonstrated the cooperation of the open Watson–Crick sites and spatial effects within the nanopores, and thermodynamic and kinetic studies revealed a hysteretic host–guest interaction attributed to mild chemisorption. We further exploited this behavior for adenine–thymine binding within the constrained pores, and a globally adaptive response of the MOF host was observed.*

The interest in designing artificial molecules and assemblies for supramolecular recognition has endured for several decades since the discovery of the archetypal Watson–Crick DNA duplex, which is sustained by nucleobase pairing.[1] Successful examples implemented include the use of natural and non-natural bases, canonical and noncanonical base-pairing patterns, and an expanding diversity of supramolecular motifs that have proved effective, such as hydrogen bonding, metal binding, dipolar interactions, and DNA bonding.[1] Many designs exploit one or a few specific motifs for binding, but the molecular entities inevitably reside in three-dimensional space (i.e. with a spatial degree of freedom of 3).[1h] The available empty room thus endorses coexisting supramolecular interactions, such as π–π stacking and hydrophobic forces, which may hamper the recognition abilities of the host–guest systems in liquid media.[1a,b] Biological DNA and RNA molecules have evolved to take advantage of spatial effects by restricting one degree of freedom through collective nucleobase pairing, and leaving the other two degrees of freedom for local twisting and folding, which in turn give rise to sophisticated adaptive behaviors, as demonstrated by DNA major-groove recognition,[2a] nucleic-acid aptamers,[2b] and adaptive materials.[2c]

Metal–organic frameworks (MOFs) are a class of crystalline porous materials that are governed by geometry in the three-dimensional assembly.[3] Their intrinsic or dynamic nanoporosity, sometimes in combination with specificity (e.g. with open metal sites), have inspired innovative developments and applications.[4] Recently, the potential of MOFs in biomimicry and biological applications has been highlighted.[5] A variety of biomolecules have been introduced as the building blocks of MOFs.[5a] Apart from a few flexible metal–peptide frameworks that mimic the conformational adaptability of proteins,[6] base-pair binding within the constrained nanospaces of nucleobase-containing MOFs or coordination polymers has rarely been explored.[5a,7]

For spatial host–guest binding within a MOF, two structural prerequisites must be fulfilled: There should be guest-accessible pores with sizes on the nanoscale, and the nucleobase residues must be immobilized on the interior surface but must leave the base-pairing sites unoccupied, that is, they must have open Watson–Crick faces (Figure 1 a). However, the low symmetry of nucleobases impedes the goal of engineering three-dimensional nanopores; in fact, most coordination polymers containing nucleobases exhibit dense crystal structures.[7b] Rosi and co-workers, among others, successfully prepared a series of highly porous adenine-based MOFs by incorporating several mono- or dicarboxylic acids as coligands.[7a,8] The most extensively studied, bio-MOF-1, possesses fully occupied N sites upon coordination with Zn,[8a] thus blocking subsequent host–guest binding. The Watson–Crick faces are exposed in bio-MOF-11 and its analogues; however, previous studies have focused on their gas-adsorption properties,[7a,8b] rather than their host–guest chemistry in liquid media. In particular, base-pair binding has not been documented in the MOF field so far.[7,16]

Herein, we report a new adenine-based MOF, namely, $Zn_3(A)(BTC)_2(H_2O)\cdot(CH_3)_2NH_2\cdot x\,DMF\cdot y\,H_2O$ (denoted as ZnBTCA; BTC = benzene-1,3,5-tricarboxyl, A = adenine, DMF = *N*,*N*-dimethylformamide), which contains a common tricarboxylic acid as a coligand. Occasionally, an adenine-free

[*] H. Cai,[+] M. Li,[+] X.-R. Lin, W. Chen, Prof. G.-H. Chen, Prof. X.-C. Huang, Prof. D. Li
Department of Chemistry and Key Laboratory for Preparation and Application of Ordered Structural Materials of Guangdong Province, Shantou University
Guangdong 515063 (China)
E-mail: dli@stu.edu.cn
H. Cai[+]
Department of Chemistry, Hanshan Normal University
Chaozhou, Guangdong 521041 (China)
[+] These authors contributed equally.

[**] This research is financially supported by the National Basic Research Program of China (973 Program, 2012CB821706 and 2013CB834803) and the National Natural Science Foundation of China (91222202 and 21171114). We are grateful for constructive criticism and suggestions from the reviewers and Prof. Jie-Peng Zhang (Sun Yat-Sen University).

Supporting information for this article is available on the WWW under http://dx.doi.org/10.1002/anie.201502045.

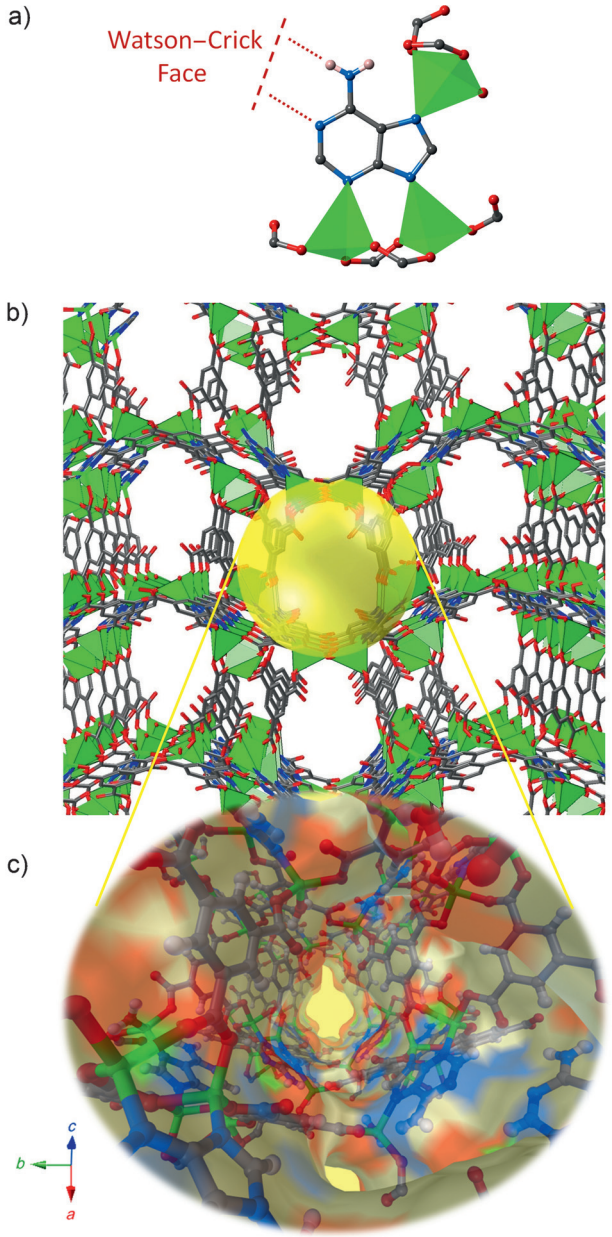

Figure 1. Open Watson–Crick sites. a) Coordination environment of adenine in ZnBTCA. b) Perspective view of the ZnBTCA framework host. c) Detailed inside view (channel region highlighted with a yellow sphere in (b)) integrated with the Connolly surface (probe radius: 1.0 Å), revealing open Watson–Crick sites on the interior surface. Color coding: C gray, N blue, O red, Zn green (shown as tetrahedra in (a,b)), H white (in (a,c)).

by-product, $Zn(BTC)\cdot(CH_3)_2NH_2\cdot DMF$[9] (denoted as ZnBTC), was obtained, but we managed to optimize the synthetic conditions to give pure crystalline samples of ZnBTCA. It was found that the interior surface of the anionic ZnBTCA framework was decorated periodically with exposed Watson–Crick faces (i.e. the adenine amino sites, and neighboring pyrimidine N sites were vacant; see the Supporting Information for experimental and structural details).[15]

The framework host ZnBTCA contains one-dimensional channels (window dimension: ca. 11 × 8 Å) running along the [101] direction (Figure 1b), thus leaving a 68.5% void volume of the unit cell defined by the Connolly surface (commonly used for visualizing the solvent-accessible surfaces of proteins, nucleic acids, and recently MOFs)[10] with a surface area of 3057.5 $m^2 g^{-1}$. The inside view of the colored Connolly surface in the channels (Figure 1c, Watson–Crick faces in blue, carboxyl O atoms in red) highlights the guest-contacting regions of the open Watson–Crick sites and the pendant carboxyl O donors. The channels are further interconnected through large windows with a diagonal dimension of approximately 10 × 10 Å, thus giving an overall three-periodic pore connectivity. The open Watson–Crick sites are aligned nearly parallel to the contacting surface, thus gating the channel-connecting windows (see Figure S1 in the Supporting Information).

To explore the host–guest chemistry of ZnBTCA, we selected a systematic set of 12 organic dyes (also used as DNA-staining agents in the context of nucleic-acids research),[2b] which differed in their ionic charge, dimensions, and contacting sites, for control experiments (Figure 2).[11] The spatial effect, attributed to the microporosity of the anionic ZnBTCA host, was demonstrated well by the negligible or limited uptake observed for the charge-mismatch and oversized groups (see Table S2 in the Supporting Information for details of the physical parameters and uptake amounts of the guests). Specifically, comparison can be made between guests with structural similarity (marked by red dotted lines in Figure 2). For example, basic and acid fuchsins ($\mathbf{BF}^+$ and $\mathbf{AF2}^{2-}$) showed distinct uptake behavior owing to a charge-complement effect. In fact, for all anionic dye guests, even for small $\mathbf{MO}^-$, the channels of ZnBTCA were inaccessible. $\mathbf{BR2}^+$, albeit bulkier, was taken up in a much greater amount than $\mathbf{NR}^0$. In the case of cationic dyes, the uptake of oversized $\mathbf{RB}^+$ and $\mathbf{R6G}^+$ was limited, whereas slightly smaller $\mathbf{R123}^+$ with amino groups was found to be adsorbed moderately. The relative uptake amounts (R_e) for those with amino groups were in the order $\mathbf{R123}^+ < \mathbf{BF}^+ < \mathbf{BR2}^+$, in accord with their decreased dimensions, thus suggesting a positive spatial effect. It was noted that $\mathbf{PfH}^+$, albeit smaller than $\mathbf{MB}^+$ and $\mathbf{BB3}^+$, exhibited a significantly lower R_e value (ca. 54 versus 99 and 96%, respectively), thus indicating that amino groups play an important role in the host–guest chemistry (see below).

Interesting hysteretic behavior was observed for the uptake of a $\mathbf{PfH}^+/\mathbf{MB}^+$ mixture as compared with the single-component curves (Figure 3). The uptake of $\mathbf{PfH}^+$ is hindered by $\mathbf{MB}^+$ at first, as evidenced by the reduced total uptake amount of $\mathbf{PfH}^+$ (ca. 38%) relative to the single-component R_e value (ca. 54%). After the adsorption equilibrium of $\mathbf{MB}^+$ has almost been reached, a second driving force causes the unusual stepwise uptake of $\mathbf{PfH}^+$, and thus its uptake plateau (at ca. 20%) displays a second drop. The release process also shows retention behavior for $\mathbf{PfH}^+$ in the presence of $\mathbf{MB}^+$ (Figure 3b). The single-component three-cycle uptake/release tests (see Figure S5) clearly indicate that $\mathbf{PfH}^+$ is not released as readily as $\mathbf{MB}^+$. All these data suggest that the second driving force responsible for the hysteretic

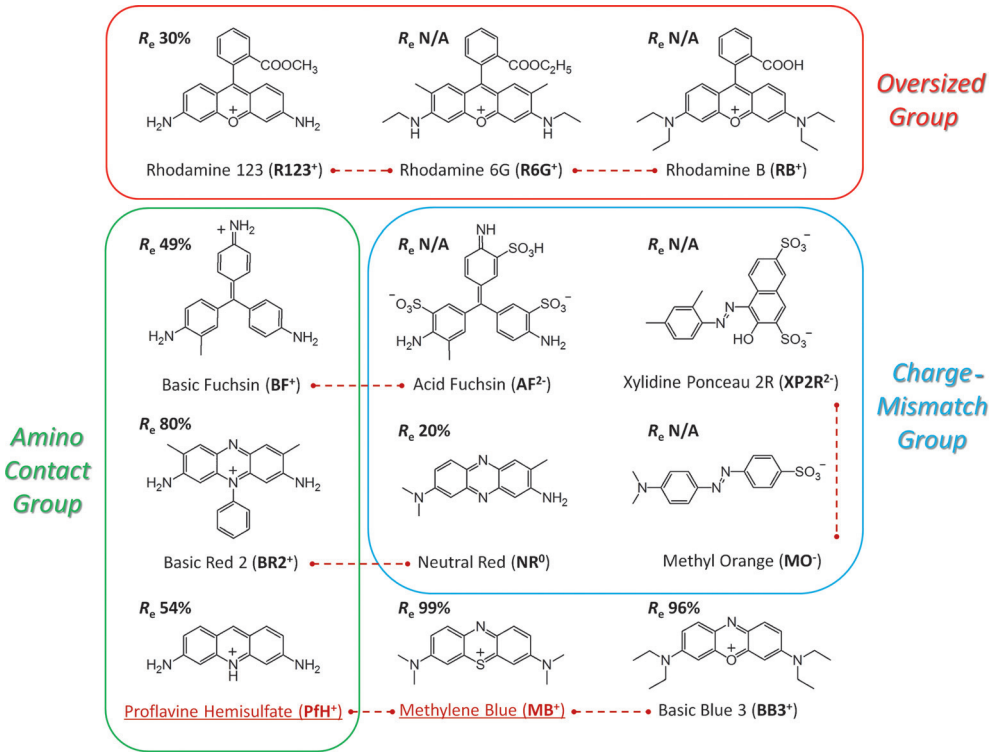

Figure 2. Variation of the guest. Organic dyes used to systematically study host–guest selectivity. The guests are grouped (in blue, red, and green boxes) to represent charge/size effects and host–guest interactions, are placed in an order roughly related to their size (larger compounds at the top and smaller compounds at the bottom), and are marked with their relative uptake amount (R_e) into ZnBTCA. The red dotted lines connect guests that are comparable in terms of structural similarity. **PfH**$^+$ and **MB**$^+$ were chosen for thermodynamic and kinetic studies.

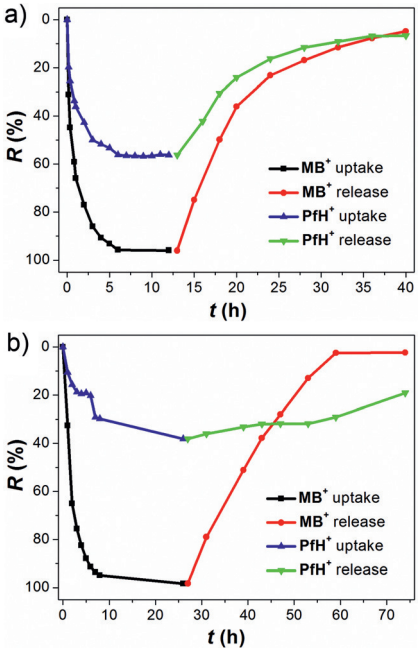

Figure 3. Hysteretic host–guest interaction. Comparison of R_t–t curves showing the guest-uptake/release behavior of ZnBTCA in a) single-component solutions of **PfH**$^+$ and **MB**$^+$, and b) a solution of an equimolar **PfH**$^+$/**MB**$^+$ mixture.

host–guest interaction for **PfH**$^+$ has an energetic profile differing in strength from the electrostatic interaction that is effective for both **PfH**$^+$ and **MB**$^+$.

To confirm that the open Watson–Crick sites contribute to the unusual uptake behavior of **PfH**$^+$, a set of complementary control experiments were designed: Now the guests were fixed (**PfH**$^+$/**MB**$^+$ mixture) while the host was varied. Three MOF hosts were studied, that is, ZnBTC,[9] ZnBTCA, and bio-MOF-1.[8a] The systematic considerations are: 1) ZnBTC (Figure 4a), ZnBTCA (Figure 4b), and bio-MOF-1 (Figure 4c) are all anionic MOFs, and thus the contributions of the charge effect are similar. 2) The pore-metrics analysis[12] of ZnBTC (Figure 4d), ZnBTCA (Figure 4e), and bio-MOF-1 (Figure 4f) can be used to visualize the spatial effect. The minimum diameters of the host channels increase in the order ZnBTC (4.386 Å) < ZnBTCA (6.066 Å) < bio-MOF-1 (9.610 Å). The greater pore-size-distribution range of ZnBTCA (ca. 2.8 Å) as compared with those of ZnBTC (ca. 1.1 Å) and bio-MOF-1 (ca. 0.1 Å) suggests that the guests may experience steric hindrance during uptake into ZnBTCA, especially considering its sinusoidal-like channel shape (Figure 4e). 3) The key difference is that only ZnBTCA possesses open Watson–Crick sites, which can potentially interact with the amino groups in **PfH**$^+$. In comparison, ZnBTC has no nucleobase coligand, whereas the Watson–Crick faces in bio-MOF-1 are blocked because of the coordination with Zn. Moreover, all three MOFs possess uncoordinated carboxyl O sites on the interior surfaces.

The above hypotheses were tested in the uptake experiments (Figure 4 g–i), and good agreement was found. First, for ZnBTC, **PfH**$^+$ takes priority with a moderate uptake amount, whereas **MB**$^+$ is limited to surface sorption, which is attributed to size exclusion because the size of **MB**$^+$ exceeds the minimum channel diameter of ZnBTC. Second, when the host channels are large enough to accommodate **PfH**$^+$ and **MB**$^+$ (as in ZnBTCA and bio-MOF-1), the uptake priority is reversed, thus indicating that the amino groups in **PfH**$^+$ may interact weakly with the MOF hosts (note that there are intruding carboxyl O donors in both ZnBTCA and bio-MOF-1), and the uptake of **PfH**$^+$ is slowed down in competition with **MB**$^+$. Moreover, the open Watson–Crick sites in

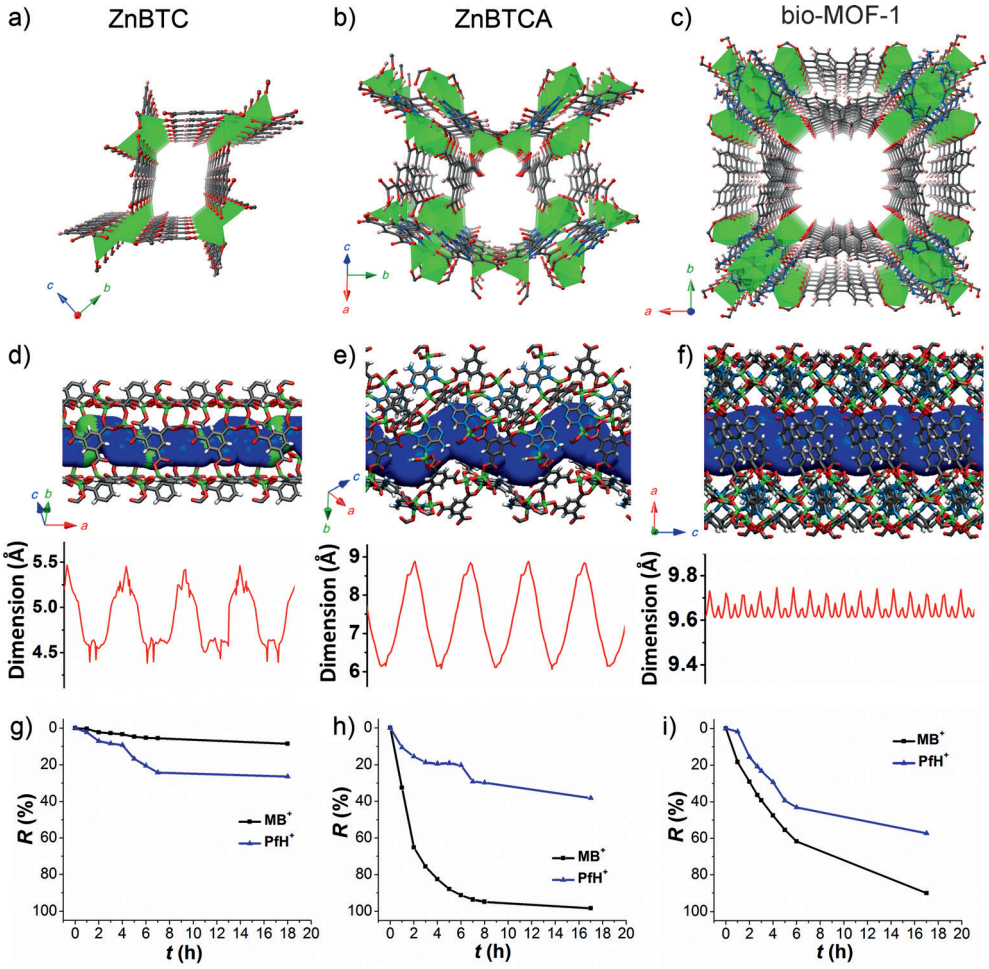

Figure 4. Variation of the host. a–c) Comparison of the top views of the accessible channels in ZnBTC (a), ZnBTCA (b), and bio-MOF-1 (c). d–f) Side views of the host channels. The shapes of the channels are highlighted by tubes in blue, and the results of pore-metrics analysis are shown (curves in red). g–i) Comparison of the uptake behavior of ZnBTC (g), ZnBTCA (h), and bio-MOF-1 (i) in solutions of an equimolar **PfH**$^+$/**MB**$^+$ mixture.

ZnBTCA further contribute to the host–guest interactions, thus giving rise to the hysteretic behavior of **PfH**$^+$, which is absent for bio-MOF-1. Third, although the channels of ZnBTCA are smaller and less uniform relative to those of bio-MOF-1, the uptake of guests appears to be much faster for ZnBTCA (Figure 4 h,i; see Figure S4 for single-component uptake curves), thus suggesting distinct sorption kinetics.

We performed thermodynamic studies[13] to quantify the energetics of the unusual host–guest interactions between ZnBTCA and **PfH**$^+$ (see the upper section of Table S3 in the Supporting Information). The results indicate that the Langmuir model is sufficient for fitting all isotherms of both **PfH**$^+$ and **MB**$^+$ adsorbed into ZnBTCA and bio-MOF-1 (see Figure S6). The positive ΔH^0 values indicate that the sorption process is endothermic, and the negative ΔG^0 and positive ΔS^0 values suggest that the spontaneous processes are mainly due to entropy effects rather than enthalpy changes. This effect is not well understood, but probably related to solvent–guest complexation, which is ubiquitous in biological systems in liquid media.[1g] The enthalpy and entropy changes in the process of the adsorption of **PfH**$^+$ into ZnBTCA are greater than the values for **MB**$^+$/ZnBTCA, **PfH**$^+$/bio-MOF-1, and **MB**$^+$/bio-MOF-1 uptake, thus distinguishing the energetic profiles of the host–guest interactions in ZnBTCA with open Watson–Crick sites.

From kinetic studies at low concentrations (see the lower section of Table S3 in the Supporting Information),[13] we conclude that the rates of uptake for both **PfH**$^+$ and **MB**$^+$ into ZnBTCA are clearly better described by pseudo-second-order kinetics.[13a] In contrast, the pseudo-first-order model gives a better fit for the kinetics of bio-MOF-1 (see Figures S7 and S8). It was proposed that for a pseudo-second-order rate mechanism, chemisorption might be significant in the rate-controlling step, whereas the pseudo-first-order model fits better for physisorption, in which the rate of the initial reaction period is crucial.[13a] The overall rate constants (k_2) for the adsorption of **PfH**$^+$ into ZnBTCA are about two to four times greater than those for **MB**$^+$, whereas the order for the initial sorption rate (h) is reversed (i.e. **PfH**$^+$ < **MB**$^+$). These factors may explain the hysteretic behavior observed for **PfH**$^+$ in the presence of **MB**$^+$ (Figure 3 b). The calculated Arrhenius activation energy (E_a) for the adsorption of **PfH**$^+$ into ZnBTCA (55.6 kJ mol^{-1}) is also much greater than that in the other three cases. It was proposed that physisorption processes usually exhibit activation energies in the range of 5–40 kJ mol^{-1}, whereas higher activation energies (40–800 kJ mol^{-1}) suggest chemisorption.[13b] Therefore, all these kinetic parameters also support the unique role of the open Watson–Crick sites in interacting with **PfH**$^+$ when it is adsorbed into ZnBTCA, thus suggesting the formation of chemical bonds of moderate strength.

On the basis of the above interesting host–guest chemistry, we envisaged that prevalent adenine–thymine (A–T) base pairing could still occur in the constrained nanospaces of ZnBTCA. It is well accepted that individual A–T binding (as opposed to the collective base pairing in DNA double strands) can only occur in aprotic solvents (e.g. $CHCl_3$ or CCl_4), rather than polar protic (e.g. H_2O or CH_3OH) and polar aprotic solvents (e.g. DMF), because hydrogen-donor/

acceptor competitors should be avoided.[1a,b] For comparison, the A–T pairing tests were performed in both $CHCl_3$ and DMF as solvents. It was found that ZnBTCA could adsorb a significant amount of thymine in $CHCl_3$ (the resulting material is denoted as ZnBTCA-T), whereas it showed almost no uptake in DMF, as expected (see Figure S9).

We were pleased to find that the host framework responded adaptively to thymine binding (Figure 5); such behavior was not observed for dye uptake, even for **PfH**$^+$ (see Figure S16a). The A–T base pairing was confirmed by the

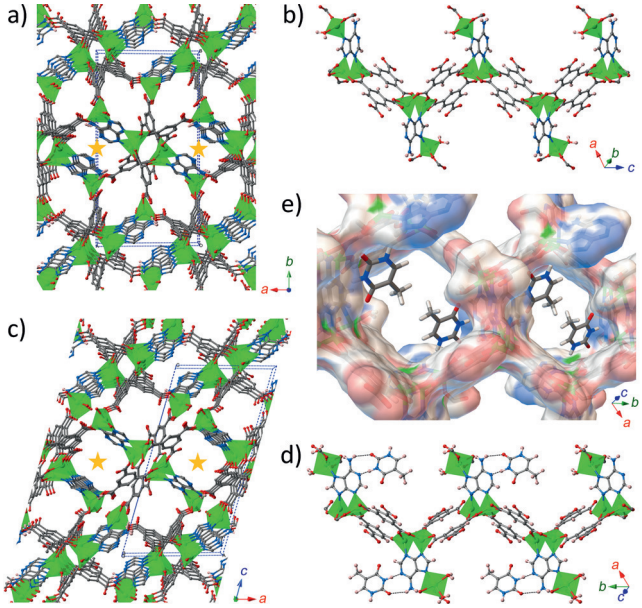

Figure 5. Adaptive host–guest recognition. Comparison of the host frameworks a,b) ZnBTCA and c–e) ZnBTCA-T. The global views (a,c) show lattice twisting (unit cells shown in blue) and the reorientation of the channel-connecting gates (marked with orange stars). The local views (b,d) show the reoriented open Watson–Crick sites pointing toward the channels after A–T binding (the thymine configuration was optimized by DFT calculations). Guest-binding pockets (e) highlighting the host–guest fitting of shape and specific binding sites (the Connolly surface of the host is colored according to polarity).

following evidence: 1) Both IR and Raman spectra (see Figures S10 and S11) showed vibrational peaks characteristic of the doubly hydrogen bonded Watson–Crick sites of A and T. 2) The subsequent dye uptake of ZnBTCA-T decreased drastically for **PfH**$^+$ but only moderately for **MB**$^+$ (see Figure S12). This result in turn confirms the host–guest interaction between **PfH**$^+$ and the Watson–Crick sites. 3) The bond parameters around the adenine Watson–Crick sites are slightly altered (see Figure S13), especially for the amino C–NH_2 bonds, which are elongated from around 1.30 (ZnBTCA) to 1.36 Å (ZnBTCA-T), very close to that (ca. 1.36 Å) for the A–T base pair in B-DNA.[14] More interestingly, half of the adenine residues reorient upon A–T binding, with the Watson–Crick sites pointing toward the channels (compare Figure 5b,d), which causes a drastic distortion of the crystal lattice (compare Figure 5a,c).[4a,b,e]

Unfortunately, the precise positions of the bound thymine could not be resolved in the X-ray diffraction study, possibly because the necessity to lower the concentration of thymine and shorten the immersion time to maintain the single crystallinity of ZnBTCA-T in $CHCl_3$ (see Figure S16b) is unfavorable for the equilibration of uptake and the formation of a periodic pattern of host–guest binding sites. On the other hand, the binding process may be affected by solvent–guest complexation, which would obscure the determination of guests, as found for the entropy-driven process in dye uptake. Further studies taking into account the solvent–guest complexation could be valuable, by analogy with insight obtained for biological systems.[1g] In this case, we instead used grand canonical Monte Carlo (GCMC) and periodic density functional theory (DFT) simulations to study the A–T binding (see the Supporting Information for computational details).

The GCMC simulations revealed that the thymine guests are distributed statistically around two major regions: the adenine Watson–Crick faces and the benzene rings in BTC, thus suggesting the host–guest interactions can be mainly attributed to base pairing and π–π stacking (see Figure S14a). We then performed DFT calculations to optimize the possible A–T binding configuration within the constrained pockets in ZnBTCA-T. Canonical Watson–Crick base pairing is disfavored owing to severe steric hindrance caused by the thymine methyl group in such a binding mode (see Figure S14b). In contrast, the reverse Watson–Crick base pairing[1b] was found to be a reasonable binding mode in ZnBTCA-T (Figure 5d). The optimized local geometry exhibits slightly longer hydrogen bonds relative to those in B-DNA,[14] thus showing a distorted pattern of the A and T planes (see Figure S14c). The energetics is compensated by additional contacts between thymine and other host sites (e.g. the carboxyl O atoms and coordinated H_2O), which lead to a quadruple-hydrogen-bonding motif for each guest. Such peripheral interactions may be responsible for the dynamic response and the shape fitting in the guest-binding pockets of the host (Figure 5e).[10] This behavior is reminiscent of the adaptive recognition of nucleic-acid aptamers,[2b] but in this case the adaption is of a global nature.

In this study, a four-stage, sequential experiment–hypothesis causality unfolded: 1) A new adenine-based MOF, ZnBTCA, was synthesized and characterized. It was envisaged that the combination of porosity and specificity (i.e. with open Watson–Crick sites) may give rise to interesting host–guest chemistry. 2) Two complementary sets of control experiments (i.e. the variation of guests with a particular host and the variation of hosts with particular guests) were designed with the aim of clarifying the spatial effect and host–guest interactions. It was then found that two of the guests had special properties in terms of sorption kinetics. 3) We then performed thermodynamic and kinetic studies to interpret the unusual hysteretic host–guest interaction. These studies revealed a unique energetic profile involving weak chemical bonding for the open Watson–Crick sites, which interact with guests bearing amino groups. 4) Although all three spatial degrees of freedom seem to be fixed in the three-periodic constrained nanospaces, the prevalent A–T base pairing confers unexpected adaptive recognition within the guest-

binding pockets, as supported by several pieces of indirect, consistent evidence. The implication of global adaptation, that is, biomimicry with periodicity, may enable the dichotomic borders that delineate biology and materials science to be stretched further.

Keywords: adaptive chemistry · host–guest chemistry · metal–organic frameworks · supramolecular recognition · Watson–Crick base pairing

How to cite: *Angew. Chem. Int. Ed.* **2015**, *54*, 10454–10459
Angew. Chem. **2015**, *127*, 10600–10605

[1] For reviews, see: a) S. Sivakova, S. J. Rowan, *Chem. Soc. Rev.* **2005**, *34*, 9; b) J. L. Sessler, C. M. Lawrence, J. Jayawickramarajah, *Chem. Soc. Rev.* **2007**, *36*, 314; c) S. Verma, A. K. Mishra, J. Kumar, *Acc. Chem. Res.* **2010**, *43*, 79; d) I. Hirao, M. Kimoto, R. Yamashige, *Acc. Chem. Res.* **2012**, *45*, 2055; e) Y. Takezawa, M. Shionoya, *Acc. Chem. Res.* **2012**, *45*, 2066; f) M. Winnacker, E. T. Kool, *Angew. Chem. Int. Ed.* **2013**, *52*, 12498; *Angew. Chem.* **2013**, *125*, 12728; g) E. Persch, O. Dumele, F. Diederich, *Angew. Chem. Int. Ed.* **2015**, *54*, 3290; *Angew. Chem.* **2015**, *127*, 3341; h) M. R. Jones, N. C. Seeman, C. A. Mirkin, *Science* **2015**, *347*, 1260901.

[2] a) M. J. Hannon, *Chem. Soc. Rev.* **2007**, *36*, 280; b) T. Hermann, D. J. Patel, *Science* **2000**, *287*, 820; c) J.-M. Lehn, *Angew. Chem. Int. Ed.* **2015**, *54*, 3276; *Angew. Chem.* **2015**, *127*, 3326.

[3] a) H. Furukawa, K. E. Cordova, M. O'Keeffe, O. M. Yaghi, *Science* **2013**, *341*, 1230444; b) M. Li, D. Li, M. O'Keeffe, O. M. Yaghi, *Chem. Rev.* **2014**, *114*, 1343.

[4] a) S. Kitagawa, K. Uemura, *Chem. Soc. Rev.* **2005**, *34*, 109; b) G. Férey, C. Serre, *Chem. Soc. Rev.* **2009**, *38*, 1380; c) K. Sumida, D. L. Rogow, J. A. Mason, T. M. McDonald, E. D. Bloch, Z. R. Herm, T.-H. Bae, J. R. Long, *Chem. Rev.* **2012**, *112*, 724; d) J.-R. Li, J. Sculley, H.-C. Zhou, *Chem. Rev.* **2012**, *112*, 869; e) J.-P. Zhang, P.-Q. Liao, H.-L. Zhou, R.-B. Lin, X.-M. Chen, *Chem. Soc. Rev.* **2014**, *43*, 5789.

[5] a) I. Imaz, M. Rubio-Martínez, J. An, I. Solé-Font, N. L. Rosi, D. Maspoch, *Chem. Commun.* **2011**, *47*, 7287; b) P. Horcajada, R. Gref, T. Baati, P. K. Allan, G. Maurin, P. Couvreur, G. Férey, R. E. Morris, C. Serre, *Chem. Rev.* **2012**, *112*, 1232; c) M. Zhang, Z.-Y. Gu, M. Bosch, Z. Perry, H.-C. Zhou, *Coord. Chem. Rev.* **2015**, *293–294*, 327.

[6] a) J. Rabone, Y.-F. Yue, S. Y. Chong, K. C. Stylianou, J. Bacsa, D. Bradshaw, G. R. Darling, N. G. Berry, Y. Z. Khimyak, A. Y. Ganin, P. Wiper, J. B. Claridge, M. J. Rosseinsky, *Science* **2010**, *329*, 1053; b) C. Martí-Gastaldo, D. Antypov, J. E. Warren, M. E. Briggs, P. A. Chater, P. V. Wiper, G. J. Miller, Y. Z. Khimyak, G. R. Darling, N. G. Berry, M. J. Rosseinsky, *Nat. Chem.* **2014**, *6*, 343; c) A. P. Katsoulidis, K. S. Park, D. Antypov, C. Martí-Gastaldo, G. J. Miller, J. E. Warren, C. M. Robertson, F. Blanc, G. R. Darling, N. G. Berry, J. A. Purton, D. J. Adams, M. J. Rosseinsky, *Angew. Chem. Int. Ed.* **2014**, *53*, 193; *Angew. Chem.* **2014**, *126*, 197.

[7] a) G. Beobide, O. Castillo, J. Cepeda, A. Luque, S. Pérez-Yáñez, P. Román, J. Thomas-Gipson, *Coord. Chem. Rev.* **2013**, *257*, 2716; b) P. Amo-Ochoa, F. Zamora, *Coord. Chem. Rev.* **2014**, *276*, 34.

[8] a) J. An, S. J. Geib, N. L. Rosi, *J. Am. Chem. Soc.* **2009**, *131*, 8376; b) J. An, S. J. Geib, N. L. Rosi, *J. Am. Chem. Soc.* **2010**, *132*, 38; c) J. An, O. K. Farha, J. T. Hupp, E. Pohl, J. I. Yeh, N. L. Rosi, *Nat. Commun.* **2012**, *3*, 604; d) T. Li, D.-L. Chen, J. E. Sullivan, M. T. Kozlowski, J. K. Johnson, N. L. Rosi, *Chem. Sci.* **2013**, *4*, 1746; e) T. Li, M. T. Kozlowski, E. A. Doud, M. N. Blakely, N. L. Rosi, *J. Am. Chem. Soc.* **2013**, *135*, 11688.

[9] L.-H. Xie, J.-B. Lin, X.-M. Liu, W. Xue, W.-X. Zhang, S.-X. Liu, J.-P. Zhang, X.-M. Chen, *Sci. China Chem.* **2010**, *53*, 2144.

[10] a) M. L. Connolly, *Science* **1983**, *221*, 709; b) M. F. Sanner, J.-C. Spehner, A. J. Olson, *Biopolymers* **1996**, *38*, 305; c) J.-H. Wang, M. Li, D. Li, *Chem. Sci.* **2013**, *4*, 1793.

[11] a) Q.-R. Fang, G.-S. Zhu, Z. Jin, Y.-Y. Ji, J.-W. Ye, M. Xue, H. Yang, Y. Wang, S.-L. Qiu, *Angew. Chem. Int. Ed.* **2007**, *46*, 6638; *Angew. Chem.* **2007**, *119*, 6758; b) Y.-Q. Lan, H.-L. Jiang, S.-L. Li, Q. Xu, *Adv. Mater.* **2011**, *23*, 5015; c) X. Zhao, X. Bu, T. Wu, S.-T. Zheng, L. Wang, P. Feng, *Nat. Commun.* **2013**, *4*, 2344; d) B.-Q. Song, X.-L. Wang, Y.-T. Zhang, X.-S. Wu, H.-S. Liu, K.-Z. Shao, Z.-M. Su, *Chem. Commun.* **2015**, *51*, 9515.

[12] a) O. S. Smart, J. M. Goodfellow, B. A. Wallace, *Biophys. J.* **1993**, *65*, 2455; b) W. Humphrey, A. Dalke, K. Schulten, *J. Mol. Graphics* **1996**, *14*, 33; c) K. C. Stylianou, J. E. Warren, S. Y. Chong, J. Rabone, J. Bacsa, D. Bradshaw, M. J. Rosseinsky, *Chem. Commun.* **2011**, *47*, 3389.

[13] a) Y. S. Ho, G. McKay, *Process Biochem.* **1999**, *34*, 451; b) B. H. Hameed, A. A. Ahmad, N. Aziz, *Chem. Eng. J.* **2007**, *133*, 195; c) E. Haque, V. Lo, A. I. Minett, A. T. Harris, T. L. Church, *J. Mater. Chem. A* **2014**, *2*, 193.

[14] H. R. Drew, R. M. Wing, T. Takano, C. Broka, S. Tanaka, K. Itakura, R. E. Dickerson, *Proc. Natl. Acad. Sci. USA* **1981**, *78*, 2179.

[15] CCDC 1047851 (ZnBTCA) and 1057226 (ZnBTCA-T) contain the supplementary crystallographic data. These data are provided free of charge by The Cambridge Crystallographic Data Centre.

[16] Note added after submission: During the reviewing process of our manuscript, two interesting new zinc adenine carboxylate MOFs were reported: a) H.-R. Fu, J. Zhang, *Chem. Eur. J.* **2015**, *21*, 5700 (this material also has potential open Watson–Crick sites, although they are not mentioned therein); b) M. Du, X. Wang, M. Chen, C.-P. Li, J.-Y. Tian, Z.-W. Wang, C.-S. Liu, *Chem. Eur. J.* **2015**, *21*, 9713 (this material has the same secondary building unit as bio-MOF-1, further linked by a tricarboxylic acid to give a mesoporous MOF).

Received: March 4, 2015
Published online: July 14, 2015

